



Seasonal dynamics of zooplankton in the southern Chukchi Sea revealed from acoustic backscattering strength

Minoru Kitamura^{a,*}, Kazuo Amakasu^b, Takashi Kikuchi^a, Shigeto Nishino^a

^a Japan Agency for Marine–Earth Science and Technology, Natsushima, Yokosuka, Kanagawa 237-0061, Japan

^b Tokyo University of Marine Science and Technology, 4-5-7 Konan, Minato-ku, Tokyo 108-8477, Japan

ARTICLE INFO

Keywords:

Acoustic backscattering strength
Chukchi Sea
Moored echo-sounder
Pelagic–benthic coupling
Seasonal changes
Zooplankton

ABSTRACT

To understand the seasonal dynamics of zooplankton in the southern Chukchi Sea, we use observations from a moored multi-frequency echo-sounder from July 2012 to July 2014. Zooplankton biomass, as indicated by area backscattering strength, was high during autumn and low in early spring; the seasonal peak in zooplankton biomass did not coincide with the spring phytoplankton bloom. This suggests that the seasonal zooplankton dynamics in the southern Chukchi Sea are less influenced by local growth of zooplankton during the spring phytoplankton bloom and more influenced by advection of zooplankton from the Bering Sea. The differences between volume backscattering strengths at 200 and 125 kHz suggest that the main acoustic scatterers are large zooplankton (euphausiids and *Neocalanus cristatus*) in late summer and autumn and small zooplankton (other copepods) in other seasons. The decrease in acoustic backscatter from large zooplankton from winter to early summer also suggests the unsuccessful overwintering of advected Pacific zooplankton. The temporal mismatch between zooplankton and phytoplankton production suggests that there is still tight pelagic–benthic coupling in the southern Chukchi Sea.

1. Introduction

The influence of climate change on the oceanic environment (e.g., increase of water temperature, shrinking ice cover, higher acidity, freshening) is evident in the Arctic Ocean (Comiso, 2011; Steele et al., 2008; Yamamoto-Kawai et al., 2009a, b). These changes affect oceanic biota in a variety of ways, such as increasing annual primary production (Arrigo et al., 2008), increasing macroalgal cover or changes in bivalve growth (Carroll et al., 2011; Kortsch et al., 2012), a northward shift of boreal fish distributions (Fossheim et al., 2015), and increasing numbers of killer whales using the Arctic as a hunting ground (Darnis et al., 2012). Such taxon-specific responses lead to speculation that the Arctic ecosystem is also changing. Tight pelagic–benthic coupling, that is, a direct connection between water-column primary production and the benthic carbon cycle resulting from low biomass in the pelagic community, is one of the characteristic features of the Arctic marine ecosystem, including the Bering Sea (Grebmeier et al., 1988; Renaud et al., 2008). The ecosystem in the northern Bering Sea, however, is shifting away from this coupling (Grebmeier et al., 2006b), whereas tight coupling is still observed in the coastal area of the Canadian Arctic (Darnis et al., 2012). It is not clear whether this coupling is still tight in other areas of the Arctic Ocean.

Low zooplankton biomass is one of the key factors contributing to tight pelagic–benthic coupling (e.g., Grebmeier et al., 1988), and zooplankton biomass is expected to be influenced by climate change. However, the number of documented changes in Arctic zooplankton is surprisingly low, and the baseline information for Arctic zooplankton is poorly understood (Wassmann et al., 2011). The seasonality of zooplankton populations—especially the timing of population increases and decreases—is one of the baseline characteristics needed to discuss whether there is still tight pelagic–benthic coupling because it will directly influence export production of organic carbon to the underlying benthos (Grebmeier, 2012). Previously, Hamilton et al. (2013) acoustically observed the seasonality of zooplankton biomass in Barrow Strait, in the eastern Canadian Arctic Archipelago. Ashjian et al. (2003) conducted yearlong zooplankton sampling to describe its abundance near ice camp SHEBA, which drifted from the Canadian Basin over the Northwind Ridge and Chukchi Plateau. However, there have been no descriptions of zooplankton seasonality in the Chukchi Sea.

In this study, we observed the seasonality of zooplankton biomass over a period of two years in the southern Chukchi Sea, which is the most productive area in the Pacific Arctic (Grebmeier et al., 2006a). To investigate any correspondence or offset in the timing of zooplankton biomass and phytoplankton blooms, observations should comprise a

* Corresponding author.

E-mail address: kitamura@jamstec.go.jp (M. Kitamura).

continuous timeseries that includes spring data. Because we had no opportunity to collect continuous and springtime data by shipboard observations, we collected data using moorings with an attached echo-sounder together with environmental sensors. There have been several sets of biological observations in the Arctic Ocean and its marginal seas using a moored acoustic device owing to its usefulness in barely accessible areas such as seasonal ice zones. However, most of these studies focused on the diel vertical migration of zooplankton (Berge et al., 2009, 2015; Cottier et al., 2006; Fisher and Visbeck, 1993; Wallace et al., 2010); descriptions of zooplankton seasonality are still rare.

Although our acoustic data include diel vertical migration signals, we do not discuss diel vertical migration in this paper. Our goals were to describe the present state of the seasonality of zooplankton biomass as baseline information and to discuss the influence of zooplankton on pelagic–benthic coupling in the southern Chukchi Sea. Acoustic backscattering strength from zooplankton and fish is known to be dependent on target size, anatomical characteristics and orientation, and the frequency of the incident sound (Lavery et al., 2007; Stanton et al., 1994). These dependences can be used to make inferences about the classification of target organisms and their size distribution (De Robertis et al., 2010; Holliday et al., 1989). Recent studies have used the differences in backscatter measurements at multiple frequencies to attempt to identify the scatterers (e.g., De Robertis et al., 2010; Lavery et al., 2007). In this study, we attempted to identify the dominant scatterers in the southern Chukchi Sea and how they are affected by the seasonal dynamics of the zooplankton community.

2. Material and methods

2.1. Study site

The Chukchi Sea is a shallow, marginal Arctic sea connected to the Bering Sea and strongly influenced by Pacific waters. Generally, the Pacific waters in the Chukchi Sea can be classified into two water types: Alaskan Coastal Water and Bering Sea Water (Coachman et al., 1975). The former is relatively warm, less saline, and more nutrient-limited, flowing on the eastern side of the Chukchi Sea with several branches flowing into the central Chukchi Sea. Bering Sea Water originates from a mixture of more saline, nutrient-rich Anadyr Water and Bering Shelf Water with intermediate salinity, entering the Chukchi Sea through the Bering Strait. The northward transport of these waters at the Bering Strait is strongest in summer and weakest in winter (Hunt et al., 2013). Along the western edge of the Chukchi Sea, the fresh, cold Siberian Coastal Current flows southward in some years and is deflected into the central Chukchi Sea (Weingartner et al., 1999). A water mass with extremely low temperature (< -1.6 °C) during winter is known as Pacific Winter Water (Pisareva et al., 2015).

Regional hydrography and marine organisms are also influenced by sea-ice dynamics. Satellite data from the Special Sensor Microwave/Imager (SSM/I) (see next section) over the last decade (2004–2014) revealed that ice melting at our mooring site starts between May and early June, whereas ice formation begins from mid-November to mid-December. Recent airborne surveys showed a mean sea-ice thickness of 2 m although extremely thick ice (> 5 m) was sometimes observed in the Chukchi Sea (Hass et al., 2010).

2.2. Mooring observations and satellite-derived data

Moorings observations were conducted at station SCH in Hope Valley in the southern Chukchi Sea from July 2012 to July 2014 (Fig. 1). To monitor the dynamics of sound scatterers, we deployed a multifrequency upward-looking echo-sounder (Acoustic Zooplankton Fish Profiler [AZFP]; ASL Environmental Sciences, Victoria, British Columbia, Canada; see Lemon et al., 2012) 7 m above the sea bottom (Table 1). To ensure continuous data collection, two identical AZFPs

were deployed alternately. Although our AZFPs collected data at 125, 200, 455, and 769 kHz, we were not able to use acoustic data from 455 or 769 kHz because of mechanical problems with the transducers.

Acoustic data were collected using the settings listed in Table 2. Acoustic sampling cell resolutions were $0.5 \text{ m} \times 30 \text{ s}$ (pings) for the first deployment and $0.2 \text{ m} \times 15 \text{ s}$ (pings) for the second and third deployments. Because the beam angle is 8° , sampling volumes were calculated as ranging from 0.1 m^3 (at 5 m from the AZFP) to 6.6 m^3 (at 10-m depth) for the first deployment and from 0.1 to 4.0 m^3 for the second and third deployments. The AZFPs were calibrated by the manufacturer before each deployment using a hydrophone and a secondary source (Lemon et al., 2012). Before the third deployment, a secondary calibration check in a tank (Lemon et al., 2012) was also performed using a 12.7-mm-diameter tungsten carbide sphere. The secondary calibration check showed calibration errors at 125 and 200 kHz of 0.8 and 0.0 dB, respectively.

Luo et al. (2000) and Hamilton et al. (2013) suggested that acoustic devices were capable of sensing organisms with minimum lengths of 1 and 0.5 mm at 153 and 307 kHz, respectively, or about one-tenth of the wavelengths. Following this suggestion, the lower detection limits for our 125 and 200 kHz AZFP would be approximately 1.2 and 0.8 mm, respectively. In contrast, Emery and Thomson (2001) noted that objects larger than about one-quarter wavelength will reflect sound, whereas objects smaller than this scatter the sound. The detectability of scatterers depends on the signal-to-noise ratio (SNR) (Furusawa et al., 1999), and a high population density of scatterers can produce a high SNR even if the individual scatterers are small.

A conductivity-temperature-depth sensor (SBE37-SM; Sea-Bird Electronics, Bellevue, Washington, USA) and a chlorophyll/turbidity sensor (INFINITY-CLW; JFE Advantech Co., Ltd, Nishinomiya, Hyogo, Japan) were attached to the AZFP frame. Environmental data were collected every hour using these sensors. For our purposes, the chlorophyll data were only used to show the timing of phytoplankton activity and as an indicator of relative chlorophyll concentrations.

Daily satellite-derived sea-ice concentration data from the SSM/I were obtained from the National Snow and Ice Data Center (<http://nsidc.org>; last accessed 7 Sep 2016). Satellite-derived sea surface temperatures (SSTs) from the Moderate Resolution Imaging Spectroradiometer were obtained from the Distributed Active Archive Center of Goddard Space Flight Center, National Aeronautics and Space Administration (<http://modis.gsfc.nasa.gov/>; last accessed 8 Sep 2016).

2.3. Acoustic data analysis

Acoustic data were converted to volume backscattering strengths (dB re 1 m^{-1}) by using the AzfpLink software (ASL Environmental Sciences, 2016). Volume backscattering strength is the logarithmic version of the volume backscattering coefficient, S_v (m^{-1}), which is the sum of the backscattering cross-section of all scatterers in the ensonified volume. For this conversion, we used calibration coefficients, sound speed, and absorption coefficients specific to each deployment. The sound speed (Mackenzie, 1981) and the absorption coefficients (Francois and Garrison, 1982) were average values calculated from conductivity-temperature-depth sensor profiles obtained near each mooring site at the beginning and end of each deployment. Files with volume backscattering strength data in comma-separated-value format created by the AzfpLink software were further analyzed using MATLAB software. The volume backscattering strength obtained includes backscatter derived from scatterers (signal) and noise as follows:

$$S_{v, meas} = 10 \log_{10} (10^{(S_{v, signal}/10)} + 10^{(S_{v, noise}/10)}), \quad (1)$$

where $S_{v, meas}$ is the volume backscatter recorded by the AZFP, $S_{v, signal}$ is the contribution from scatterers, and $S_{v, noise}$ is the contribution from noise (De Robertis and Higginbottom, 2007). The

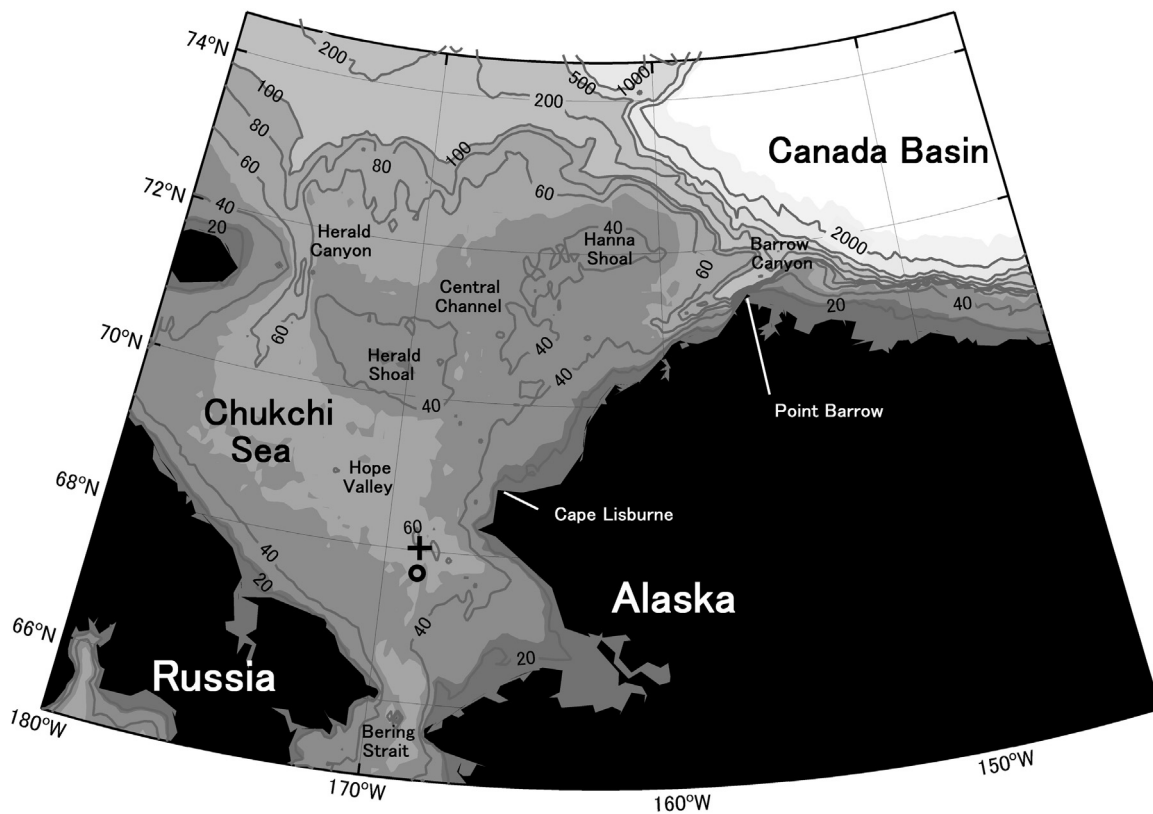


Fig. 1. Bathymetry and mooring locations in the southern Chukchi Sea. The open circle shows the location of mooring SCH-12-1 and the cross shows that of SCH-12-2 and SCH-13.

Table 1
Mooring configurations.

Mooring	Latitude (N)	Longitude (W)	Bottom depth (m)	AZFP ^a depth (m)	Period
SCH-12-1	67°42.18′	168°50.01′	52	45	16 July–2 Oct 2012
SCH-12-2	68°02.00′	168°50.03′	59	52	3 Oct 2012–20 July 2013
SCH-13	68°02.00′	168°50.03′	60	53	20 July 2013–19 July 2014

^a Acoustic Zooplankton Fish Profiler.

Table 2
Acoustic Zooplankton Fish Profiler (AZFP) settings.

AZFP parameter	Moorings	
	SCH-12-1	SCH-12-2, SCH-13
Burst interval (s)	60	120
Ping period (s)	1	2
Pulse length (ms)	0.5	0.3
Digitization rate (kS s ⁻¹)	20	20
Number of pings per burst interval	30	15
Bin thickness (m) (average number of samples)	0.5 (13)	0.2 (5)
Maximum recording range from the transducer (m)	103	101

noise can be described as a function of distance from the AZFP (m):

$$S_{v,noise} = 20\log_{10}R + 2\alpha(R-1) + \text{offset}, \tag{2}$$

where R is the distance, α is the absorption coefficient, and “offset” is a constant. In this study, the offset was determined by using the backscattering strength recorded at distances of 70–90 m (first deployment) or 60–80 m (second and third deployments) through a least-

squares estimation technique. Because the area at 60–90 m from the AZFP is located above the sea surface, echo signals collected from there are identifiable as noise. Then $S_{v,signal}$ was calculated as follows:

$$S_{v,signal} = 10\log_{10}(10^{(S_{v,meas}/10)} - 10^{(S_{v,noise}/10)}). \tag{3}$$

Although this provides a theoretical method for removing noise, misinterpretations are possible when analyzing weak signals against noise. Thus, we applied an echo threshold by using the SNR (dB), which can be estimated as follows (De Robertis and Higginbottom, 2007):

$$\text{SNR} = S_{v,signal} - S_{v,noise}. \tag{4}$$

In this study, we accepted and used for further analysis $S_{v,signal}$ cells with an SNR greater than 10 dB. For $S_{v,signal}$ below the threshold value, a value of -999 was used as $S_{v,signal}$ instead of zero, because the logarithm of zero is undefined, whereas -999 produces an approximation of zero on a linear scale (De Robertis and Higginbottom, 2007).

To understand the dynamics of sound scatterers, we produced echograms of $S_{v,signal}$ (hereafter “ S_v ”) from the three deployments. We also obtain the area backscattering coefficient (s_a , m² m⁻²) which is a vertical integration of the volume backscattering coefficient (s_v) over the sampled depth interval, and is proportional to scatterer biomass. The area backscattering strength (S_a , dB re 1(m² m⁻²)) which is the logarithmic form of s_a , is also useful, since it better reveals seasonal patterns in periods of relatively low biomass. To obtain s_a , volume backscattering coefficients (s_v), which are S_v on a linear scale, were vertically integrated over the depth range of 10–40 m (first deployment) or 10–47 m (second and third deployments) and averaged over the time periods of 1000–1200 and 2200–2400 UTC. These time periods were local nighttime and daytime, respectively (midnight and midday at the mooring site were 1100 and 2300 UTC, respectively). Thereafter, the s_a values were converted to the decibel scale (S_a). Backscattering data for the upper 10 m were excluded because of

extremely strong echoes, which were probably due to seasonal sea ice or air bubbles produced by breaking waves. The lower limit of the integration was set to 5 m above the AZFP to exclude noise in the depth range near the AZFP. For the third deployment, the lower limit was set to 6 m above the AZFP for comparison with the second deployment. Because our acoustic observations did not cover the entire water column, the obtained backscattering strengths should be considered underestimates of the strengths that would have been obtained from the entire zooplankton community at the mooring site. A likely important source of error is the missing observations from the top 10 m, which was a highly productive layer. However, the goal of the present study was to examine seasonal patterns of zooplankton dynamics rather than establishing quantitative estimates of zooplankton populations.

By using two sound frequencies (125 and 200 kHz), we also attempted to differentiate between general classes of scatterers. Using the distorted-wave Born approximation-based prolate spheroid model (Chu and Ye, 1999), we estimated theoretical target strengths against frequencies for zooplankton (copepods and euphausiids) and fish without a swim bladder (“non-swim-bladder fish”). We also estimated the theoretical target strengths of fish with a swim bladder (“swim-bladder fish”) using the modal-series-based prolate spheroid model (Furusawa, 1988). The model parameters are listed in Table 3. We also determined the relationships between $\Delta TS_{200-125}$ (target strength at 200 kHz minus target strength at 125 kHz) and body lengths for zooplankton and fish and attempted to differentiate between general classes of scatterers by using $\Delta TS_{200-125}$. If we assume that a single type of scatterer dominated a depth cell of the acoustic sampling, then $\Delta S_{v200-125}$ in the depth cell is independent of scatterer's number and is equal to $\Delta TS_{200-125}$ of the scatterer (Kang et al., 2002). We used this assumption and $\Delta S_{v200-125}$ to estimate the major scatterers in the water column at the mooring site.

2.4. Zooplankton sampling

To identify the possible main scatterers, it was necessary to obtain information about the dominant taxa in the zooplankton community and their size distributions. We sampled zooplankton around station SCH in September and early October 2012 and in July 2013 (Table 4). A conical net (80-cm mouth diameter, 335- μ m mesh size) equipped with a calibrated flow meter was hauled vertically from the AZFP mooring depth to the sea surface at a speed of 1 m s⁻¹. Net samples were fixed and preserved in a 5% formalin solution buffered with sodium tetraborate. Zooplankton were sorted from the preserved

Table 3

Model parameters for estimating target strength of potential scatterers. DWBA-PSM and MS-PSM are abbreviations for “distorted-wave Born approximation-based prolate spheroid model” and “modal-series-based spheroid model”, respectively. Lengths are prosome length for copepods and body length for others. Aspect ratios (body width or height: body length) were determined for zooplankton by measuring collected specimens and for fish using data from Furusawa (1988). Contrast is the ratio between the animal's density and that of the surrounding seawater, or between the sound speed through the animal and that through the surrounding seawater. These contrasts are cited from literature. The orientation distribution for each animal is shown as an average orientation angle (degrees) and a standard deviation. An angle of 0° indicates horizontal orientation and corresponds to ventral incidence.

Scatterer	Model	Length (mm)	Aspect ratio	Contrasts		Orientation distribution (mean, SD)
				Density	Sound speed	
Copepoda	DWBA-PSM	0.5–1.4	0.38	1.005 ^b	1.007 ^b	(0, 30) ^d
		1.5–7	0.30	1.005 ^b	1.007 ^b	(0, 30) ^d
Euphausiacea	DWBA-PSM	1–4	$-0.15\log_e(L)+0.35$	1.018 ^b	1.006 ^b	(0, 27.3) ^c
		5–26	0.14	1.018 ^b	1.006 ^b	(0, 27.3) ^c
Swim-bladder fish	MS-PSM	10–150	0.15 ^a	–	–	(0, 10) ^a
Non-swim-bladder fish	DWBA-PSM	10–150	0.15 ^a	1.021 ^c	1.018 ^c	(23.3, 25.4) ^f

^a Furusawa (1988).

^b Smith et al. (2010).

^c Yasuma et al. (2009).

^d Lawson et al. (2004).

^e Lawson et al. (2006).

^f Kubilius and Ona (2012).

Table 4

Locations of net sampling sites. Zooplankton were collected by vertical hauls of a conical net (80-cm mouth diameter, 335- μ m mesh).

Station	Date	Latitude (N)	Longitude (W)	Sampling depths (m)
7	13 Sep 2012	67°30′	168°45′	42–0
8	14 Sep 2012	67°45′	168°30′	42–0
15	14 Sep 2012	68°00′	168°45′	50–0
86	3 Oct 2012	68°07′	168°45′	51–0
89	3 Oct 2012	68°00′	168°45′	52–0
OS13124	16 July 2013	67°38′	168°57′	45–0

samples into the following 13 major taxa: Cnidaria, Ctenophora, Polychaeta, Mollusca, Cirripedia, Copepoda, Amphipoda, Ostracoda, Euphausiacea, Decapoda, Cumacea, Chaetognatha, and Appendicularia. The sorted animals were counted, measured for body length and width, dried for 24 h at 60 °C after removing interstitial water by filtration, and then weighed on an electric balance (GR-202, A & D Company, Ltd., Tokyo, Japan). From these data, we determined the major taxa comprising the community on the basis of dry mass and size distributions of the dominant taxa.

3. Results

3.1. Seasonality of environmental properties

During the first winter, sea ice started appearing in mid-November 2012 and started breaking up in late May 2013. In contrast, ice formation in the second winter was one month later than in the first, and the breakup started in early May (Fig. 2a). Sea-ice concentrations through the second winter were relatively low (observed at 53% on 1 February 2014); the mean concentration between January and March was 82%, whereas in the first winter it was 97%. The ice concentration anomaly revealed that (1) freezing began earlier in the first winter and later in the second winter compared with the average date of freezing from 2004 to 2014, (2) ice concentrations in the second winter were lower than the average concentrations, and (3) ice melting started earlier in the second spring than the 10-year average (Fig. 2b).

Satellite-derived SSTs ranged between -0.73 and 7.54 °C; the lowest observed temperature was in November 2012 just before sea-ice formation and the highest was in August 2013 (Fig. 2c). SSTs decreased after mid- or late August and the water column became vertically well-mixed in October of both years. Monthly mean SST in

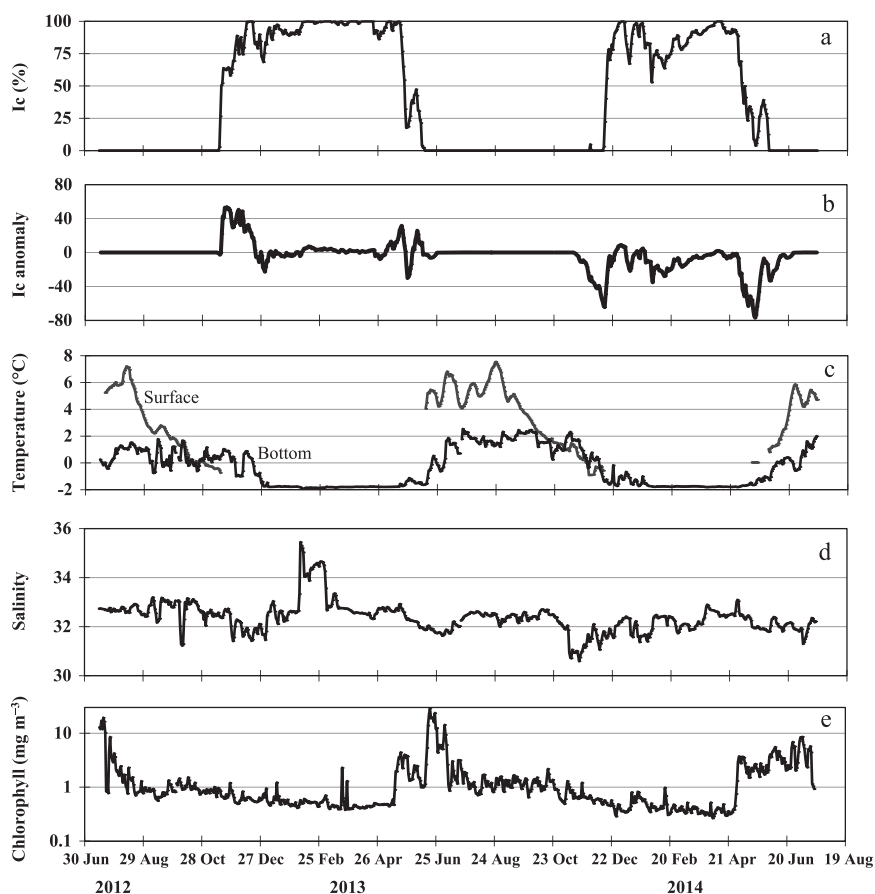


Fig. 2. Seasonal changes of environmental properties from 16 July 2012 to 19 July 2014 in the southern Chukchi Sea. (a) Ice concentration (I_c , %), (b) ice concentration anomaly, (c) water temperature at sea surface and bottom layer ($^{\circ}\text{C}$), (d) bottom-layer salinity, (e) chlorophyll concentration (mg m^{-3}). The ice concentration anomaly is the difference between observed concentration and average concentration from 2004 to 2014. Bottom layer water temperature, salinity, and chlorophyll concentration were observed 7 m above the sea bottom. Note the logarithmic scale for the vertical axis of chlorophyll concentration in (e). Note also that the chlorophyll information should only be considered an indicator of phytoplankton seasonality.

October 2013 (1.9°C) was higher than that in October 2012 (0.6°C), and the SST during autumn probably affected the sea-ice extent and the timing of freeze-up. Bottom temperatures ranged between -1.92 and 2.53°C during the two years of observation and were stable at about -1.8°C from mid-winter to spring (late April or mid-May; Fig. 2c). Temperatures and salinities (Fig. 2d) indicated a water mass similar to Bering Sea Water from summer to autumn, and Pacific Winter Water was present from winter to early spring in the bottom layer. Shipboard observations showed a strong stratification in September 2012 caused by the high fraction of sea-ice meltwater at the surface at the study site (Nishino et al., 2016). Chlorophyll concentration rapidly increased when sea ice started breaking up in May, and high concentrations continued until July (Fig. 2e). During the post-bloom period until late October or early November, chlorophyll concentrations were relatively high compared with those in winter; low concentrations were observed between January and April. Details of the water-mass characteristics at the mooring site have already been reported (Nishino et al., 2016).

3.2. Seasonal change of AZFP backscattering strength

Results at 125 kHz and 200 kHz reveal a similar pattern (Fig. 3). High S_v values occur starting in mid to late July in both years. In 2012 S_v begins declining starting in mid-October, particularly at the surface, but in 2013 high values persist well into November. From winter to early summer, S_v values at 200 kHz were higher than those at 125 kHz.

Temporal changes in S_a and s_a at 125 and 200 kHz are shown in Fig. 4. Because the values and temporal trends were similar for daytime

and nighttime S_a and s_a , in this section we describe the seasonal variability of backscattering strengths on the basis of nighttime data. There were high S_a and s_a values at both 125 and 200 kHz in late summer and autumn, whereas both parameters had low values in late winter and early spring. This suggests that the biomass of scatterers was still low during the spring phytoplankton bloom from May to June. On the other hand, the differences between the S_a values at 125 and 200 kHz were small in autumn (average 1.0 dB) whereas they were large in spring (6.9 dB). S_a values at 200 kHz were larger than those at 125 kHz during the two seasons. Since small zooplankton may not be reliably with the lower frequency, these observations suggest that the dominant size of zooplankton changed from large (autumn) to small (spring).

After the autumn periods with high S_a , there were sudden decreases in S_a at different times in the two years: mid-November in 2012 and early December in 2013. The sudden decrease in the first year coincided with the timing of freeze-up, although in the second year the decrease came a half month before the freeze-up of seasonal sea ice. During the month before the sudden decrease of S_a , SSTs were relatively constant between 0 and -0.5°C in 2012, whereas those in 2013 were variable between 1.5 and -0.9°C . At the same time, bottom water temperatures were also constant in 2012 but decreasing in 2013. There were no observed temporal changes in chlorophyll concentration leading up to the S_a decrease in either year. Daytime lengths during the periods of S_a decrease were also different each year (about 5 h in 2012 and 1 h in 2013); this has been suggested as a trigger for changes in zooplankton physiology such as diapause (Marcus, 1984; Norrbin, 1996). The sudden decrease in S_a suggests a decrease in zooplankton

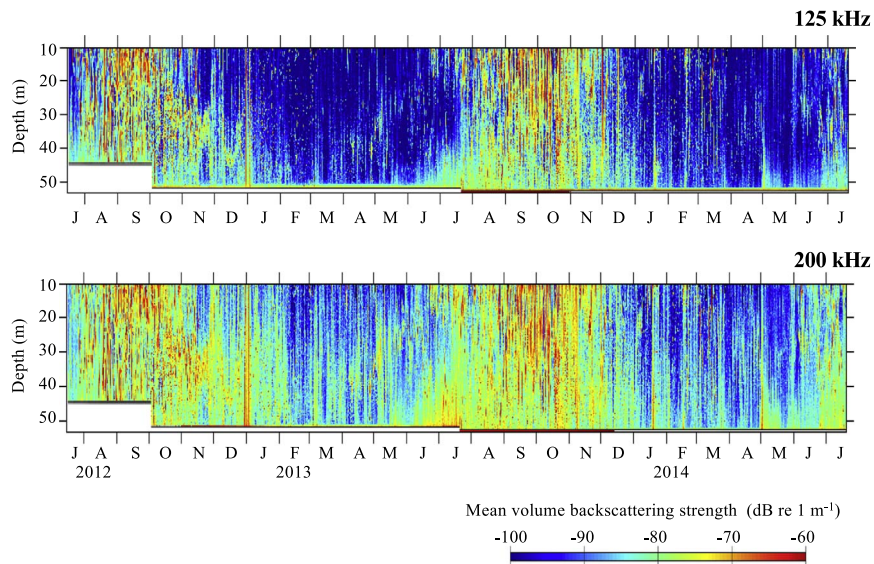


Fig. 3. Seasonal changes in mean volume backscattering strength (S_v , dB re 1 m^{-1}) observed by using a moored Acoustic Zooplankton Fish Profiler (AZFP) at station SCH in the southern Chukchi Sea from 16 July 2012 to 19 July 2014. The top and bottom panels show echograms at 125 and 200 kHz, respectively.

biomass triggered by environmental factors; however, we could not identify the factor(s).

In contrast, the timing of the increase in S_α during the spring was similar in the two years (mid-May in 2013 and late May in 2014). The

increase in S_α coincided with an increase in water temperature in the bottom layer (Fig. 5a, b, e, f), and the rate of S_α increase was higher in 2014 when that of water temperature in the bottom layer was higher compared with 2013. Chlorophyll concentration increased before the

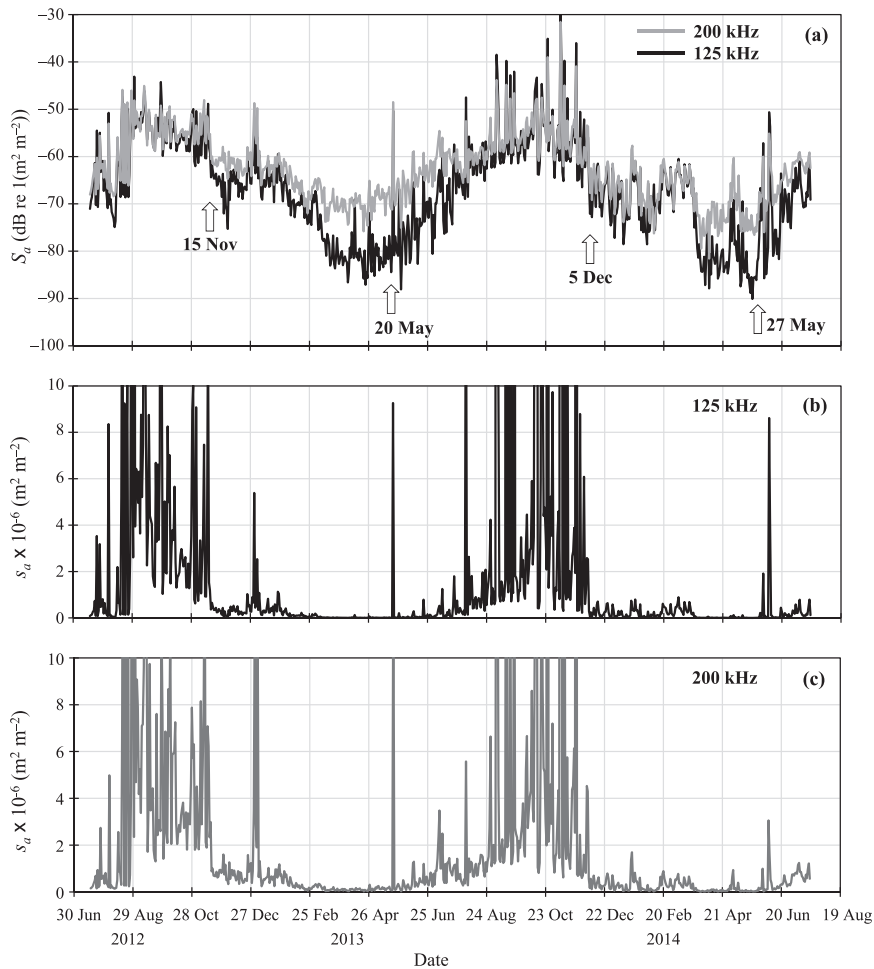


Fig. 4. Seasonal changes in area backscattering strengths (S_α , dB re $1(\text{m}^2 \text{ m}^{-2})$) and area backscattering coefficients (s_α , $\text{m}^2 \text{ m}^{-2}$) observed by using a moored Acoustic Zooplankton Fish Profiler (AZFP) in the southern Chukchi Sea. Note that S_α is defined as a $10\log_{10}$ value whereas s_α is linearized S_α and is nearly proportional to scatterer biomass. (a) S_α at 125 kHz (black) and 200 kHz (gray), (b) s_α at 125 kHz, and (c) s_α at 200 kHz. Arrows in (a) indicate the start of rapid decreases in S_α in early winter and increases in spring.

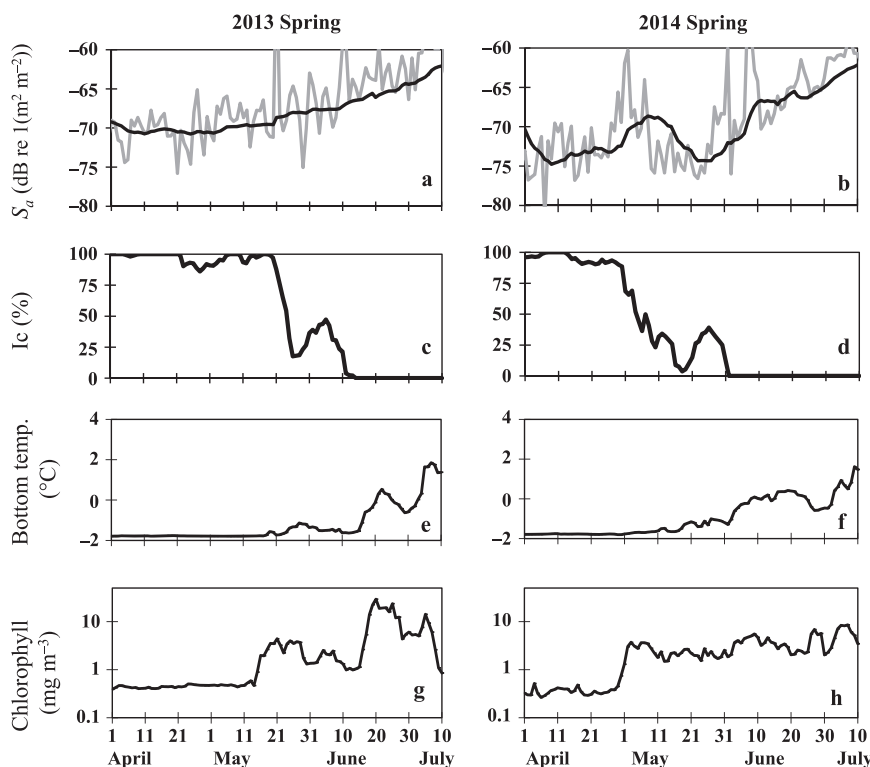


Fig. 5. Temporal changes in area backscattering strength (S_{α}) and environmental properties during the time of S_{α} increase in the first and second springs of the study period. (a, b) S_{α} at 200 kHz and running means (30 days) (dB re $1(\text{m}^2 \text{m}^{-2})$); (c, d) ice concentration (%); (e, f) water temperature in the bottom layer ($^{\circ}\text{C}$); (g, h) chlorophyll concentration (mg m^{-3}). Left panels show data for spring 2013 and right panels are for spring 2014.

increase in S_{α} in both springs (Fig. 5g, h); however, the S_{α} increase seemed to be independent of the seasonal breakup of sea ice. Specifically, the sea-ice reduction and S_{α} increase coincided in May 2013, whereas the breakup of sea ice in 2014 was observed about a month before the S_{α} increase in May (Fig. 5a–d).

3.3. Community structure and size-range of zooplankton in summer and autumn

Around the mooring site, copepods and euphausiids were dominant in the zooplankton community from summer to autumn (Fig. 6). Copepods accounted for 55.5–81.2% of the total biomass in July and September, whereas their relative biomass decreased to 29.2% in October. Conversely, the relative biomass of euphausiids increased from July to October, with a maximum of 52.0% of the total biomass at station 89. Because zooplankton were sampled by vertical hauls of a conical net, the biomass of euphausiids could have been underestimated because of their net avoidance. In the copepod community, small copepods below 2 mm in prosome length were the most abundant throughout the sampling period, whereas abundances of larger copepods (≥ 2 mm) were relatively high in September compared to other months. A large (≥ 7 mm) Pacific copepod, *Neocalanus cristatus*, was also collected in September, but in low abundance. All euphausiids collected in July were small (≤ 3.2 mm in body length) and in early life stages, such as calyptopsis larvae, whereas large euphausiids (≤ 26.5 mm) were collected in autumn. Barnacle larvae (< 1.2 mm in length) were abundant in July and they accounted for 25% of the zooplankton community biomass. Amphipods sometimes showed high biomass in September and October ($\leq 22.7\%$ of the total zooplankton biomass) and several specimens were greater than 10 mm in body length.

3.4. Main organisms responsible for acoustic scattering

Potential scatterers in the southern Chukchi Sea would include zooplankton and fish. Plankton-net samples from around the mooring site suggest that the main zooplankton scatterers were Copepoda and Euphausiacea (Fig. 6). Because Pacific herring, *Clupea pallasii* (mean length, 20 cm), and chum salmon, *Oncorhynchus keta* (19.6 cm), dominate the pelagic fish community in the southern Chukchi Sea during autumn (Eisner et al., 2013), these swim-bladder fish species were also considered as potential scatterers. Although siphonophores with a gas-filled pneumatophore are generally recognized as acoustic scatterers (Lavery et al., 2007; Stanton et al., 1994), they have not been recorded from the shallow Chukchi Sea (Ronowicz et al., 2015) and were not collected in our net samples. Presumably, this taxon is not distributed in the Chukchi Sea. A large medusa of the Pacific scyphozoan *Chrysaora melanaster* was observed in the Pacific water in the Canada Basin (Purcell et al., 2010), so this species was also considered a potential scatterer at our mooring site.

We estimated theoretical target strengths against frequencies for zooplankton (copepods and euphausiids) and fish; the results for selected sizes are presented in Fig. 7. We used these estimations to determine the relationships between $\Delta TS_{200-125}$ and body lengths for zooplankton and fish (Fig. 8). Most of the zooplankton size classes had positive $\Delta TS_{200-125}$ values, although the largest euphausiids (> 25 mm) had negative values; larger zooplankton had lower values. $\Delta TS_{200-125}$ values of swim-bladder fish were negative (near 0 dB) for all size classes. For non-swim-bladder fish, $\Delta TS_{200-125}$ was variable from -4 to $+5$ dB; two size classes (< 2 and ~ 5 cm) had positive values similar to the euphausiids. Although shorthorn sculpin, *Myoxocephalus scorpius*, was in the latter size class and was found around the study site, its contribution to the acoustic backscattering strength was thought to be small because of its low abundance (Eisner et al., 2013). The lowest $\Delta TS_{200-125}$ was in non-swim-bladder fish with a body length of about 3 cm, and the $\Delta TS_{200-125}$ of larger non-swim-

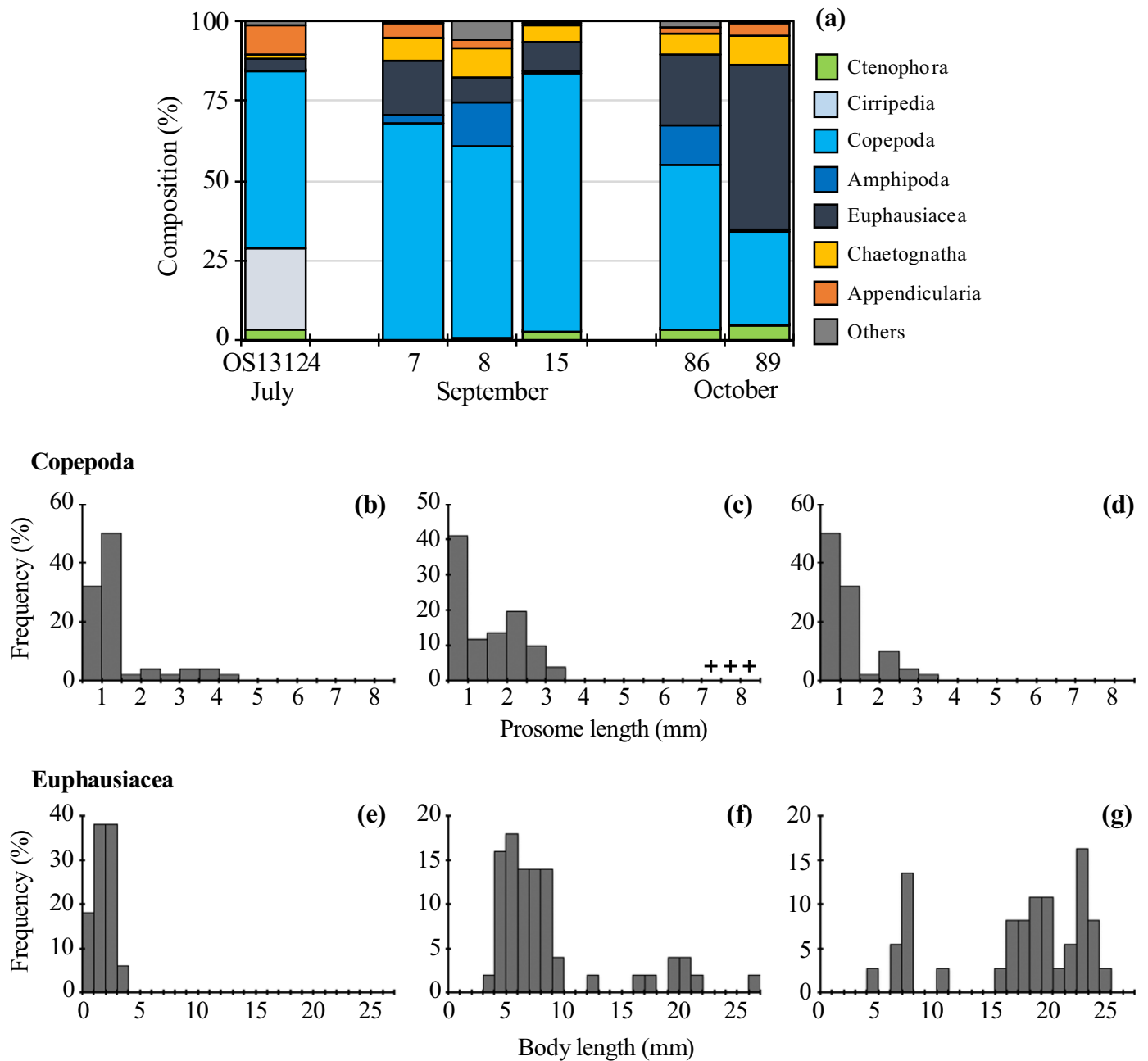


Fig. 6. Composition of zooplankton community by major taxa, based on dry weight, in samples from six stations around the mooring sites (a). Size distributions of two dominant taxa: Copepoda (b–d) and Euphausiacea (e–g). Size distributions of the two taxa are from samples collected at station OS13124 in July 2013 (b, e), at station 7 in September 2012 (c, f), and at station 89 in October 2012 (d, g), respectively. Net sampling was conducted around the mooring sites by vertical hauls of a conical net (80-cm mouth diameter, 335- μ m mesh size).

bladder fish (> 6 cm) converged on 0 dB.

If we assume that a single species of scatterer dominated a depth cell of the acoustic sampling, then $\Delta S_{v200-125}$ in the depth cell is equal to $\Delta TS_{200-125}$ of the scatterer (Kang et al., 2002). Based on this assumption, we divided AZFP acoustic signals into three categories: (1) signals derived from small zooplankton ($\Delta S_{v200-125}$ over 5 dB), (2) signals from large zooplankton including larval non-swim-bladder fish (from 0 to 5 dB), and (3) signals from fish, excluding larval non-swim-bladder fish, and the largest size class of euphausiids (> 25 mm) (from 0 to -5 dB). Most of the copepod species (< 6 mm in length) and early-stage euphausiids (< 10 mm) were categorized as small zooplankton. The large zooplankton included the Pacific copepod *N. cristatus* (~ 7 mm) and euphausiids at later developmental stages (10–25 mm), although *N. cristatus* was not abundant in our net samples. The third category with $\Delta S_{v200-125}$ less than 0 dB included the largest size class

of euphausiids (> 25 mm). Although our net samples suggested these as a minor group in the euphausiid community ($\leq 2\%$ by abundance, Fig. 6), their abundances may have been underestimated because of net avoidance. Thus, their contribution to the third category is still uncertain. The classification of scatterers might also have uncertainties derived from calibration errors and uncertainty of model parameters, such as changes in animal swimming orientation, or the accuracy of the acoustic scattering models.

According to the $\Delta S_{v200-125}$ categorization, the $\Delta S_{v200-125}$ echogram and frequency distributions (Fig. 9) suggest that the main scatterers in the southern Chukchi Sea were large zooplankton, including larval non-swim-bladder fish, from mid-summer to autumn, whereas small zooplankton were dominant from winter to early summer. This characterization of scatterers is consistent with the compositions in terms of major taxa in July and October but is not

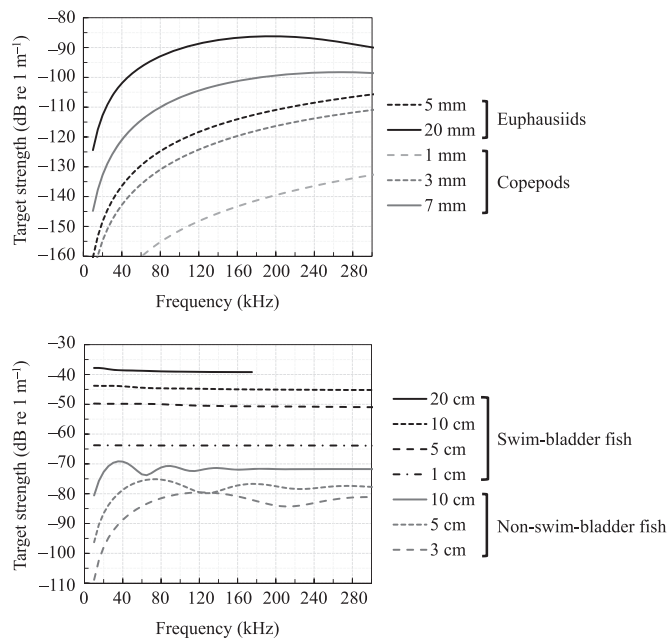


Fig. 7. Theoretical target strength as a function of frequency for selected size classes of dominant zooplankton (top panel) and fish (bottom panel).

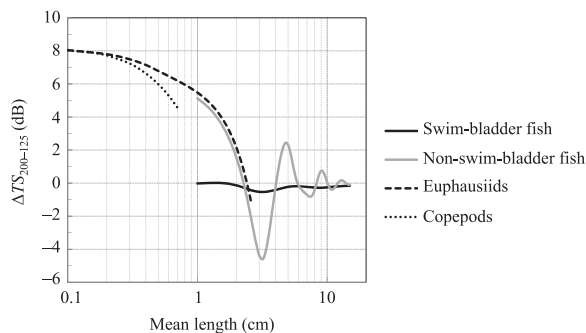


Fig. 8. Decibel differences between target strengths at 200 and 125 kHz ($\Delta TS_{200-125}$) as a function of mean body length for four groups of scatterers: copepods, euphausiids, and fishes with and without a swim bladder.

consistent with that in September (Fig. 6). This inconsistency might be at least partially explained by the fact that net samples were collected near the mooring site, but not right at the site, and that biomass estimates of larger zooplankton based on net samples tend to be underestimates because of net avoidance. Further studies involving sample collections are needed for the zooplankton fauna, especially for the larger species.

4. Discussion

4.1. Key factors affecting zooplankton dynamics in the Chukchi Sea

In this study, peak zooplankton biomass in the Chukchi Sea as indicated by S_a was in autumn and did not coincide with the spring phytoplankton bloom. In contrast, an earlier study found peak zooplankton biomass in the Bering Sea during spring, except in the northwestern coastal area where sea ice persisted during spring (Stafford et al., 2010; Volkov, 2008). This earlier study also showed that the timing of the peak biomass coincided with the phytoplankton bloom. This difference in zooplankton seasonality between the two seas suggests a smaller contribution of local zooplankton growth during the spring phytoplankton bloom to the seasonal variability of zooplankton biomass in the southern Chukchi Sea.

The hydrography of the Chukchi Sea is strongly influenced by the

advection of water masses from the Bering Sea (Grebmeier et al., 2006a), and this advection is relatively strong in summer and weak in winter (Hunt et al., 2013). In the Bering Sea, intermittent high zooplankton biomass has been observed throughout the warm period (Stafford et al., 2010). Our observed $\Delta S_{v200-125}$ suggests that the main scatterer during autumn was large zooplankton such as euphausiids, whose stock in the Chukchi Sea is considered to be maintained through the input of new individuals from Bering Sea stock (Springer et al., 1989). This suggests that the observed high S_a during autumn in the southern Chukchi Sea was largely due to a direct increase in biomass by zooplankton transported from the Bering Sea. Thus, the most important factor affecting the seasonal variability of zooplankton biomass in the southern Chukchi Sea is probably the advection of the zooplankton community from the Bering Sea. This conclusion is supported by Weingartner (1997), who suggested that secondary production in the Chukchi Sea is largely due to northward transport of zooplankton from the Bering Sea.

It is still unclear whether larger Pacific zooplankton can overwinter in the Arctic Ocean. However, the clear decrease in acoustic data derived from larger zooplankton between winter and early summer (Fig. 9) suggests their unsuccessful overwintering. Among the Pacific species, *Neocalanus* spp. together with *Calanus marshallae* are dominant in the Chukchi Sea (Hopcroft et al., 2010), and these copepods enter diapause during winter in the subarctic Pacific and the Bering Sea (Geinrikh, 2002; Miller et al., 1984; Smith and Vidal, 1986). However, the low water temperature in the Chukchi Sea probably prevented their successful overwintering there. For example, wintertime water temperatures in the southern Chukchi Sea (as low as -1.8°C) were lower than those at the depths of dormant *Neocalanus* spp. in the subarctic Pacific ($\approx 3^\circ\text{C}$; Kobari and Ikeda, 1999; Miller et al., 1984). Although *Thysanoessa* spp., which are considered advected Pacific euphausiids, may live for 2–4 years in subarctic waters (Astthorsson and Gislason, 1997; Falk-Petersen and Hopkins, 1981), our acoustic time-series data likewise suggest their unsuccessful overwintering in the southern Chukchi Sea.

Our acoustic results also revealed that small zooplankton were dominant but decreasing in biomass during winter (Figs. 4 and 9), and $\Delta S_{v200-125}$ echograms show a deepening of the distribution of small zooplankton from late autumn to winter (Fig. 9). This suggests the possibility that the small zooplankton migrated downward and some or most of their populations left the observation depths of the AZFP (moored 7 m above the bottom). It is likely that the small zooplankton migrated downward not only at the mooring site but also in the upstream area, and they were advected from the upstream area into the mooring site. In the Chukchi Sea, the small endemic Arctic copepods *Calanus glacialis* and *Pseudocalanus* spp. were reported as dominant species (Hopcroft et al., 2010), and they migrate downward for diapause during winter (Ashjian et al., 2003; Conover and Siferd, 1993; Falk-Petersen et al., 2009; Norrbin, 1994). As in our study, Hamilton et al. (2013, Fig. 4d) reported that the vertical distribution of zooplankton deepens from late autumn to winter in the Canadian Arctic Archipelago.

At station SCH, the spring S_a increase started in late May in both years. The increase corresponded not with sea-ice retreat but with the increase of water temperature in the bottom layer (Fig. 5). Because we found higher S_v in the deeper water column during late May (Fig. 3), it seems reasonable that environmental properties in the bottom layer affect zooplankton dynamics during spring. There is also a weak relationship between the dates of zooplankton increase and ice breakup in the Canadian Arctic Archipelago (Hamilton et al., 2013). In our study, the response of S_a to the phytoplankton bloom was slightly different in the two springs: S_a increased just after the start of the phytoplankton bloom in the first spring, whereas S_a increased about a month after the initiation of the bloom in the second spring. Thus, the phytoplankton bloom alone did not seem to be a trigger for the S_a increase, although the spring bloom starting prior to the zooplankton

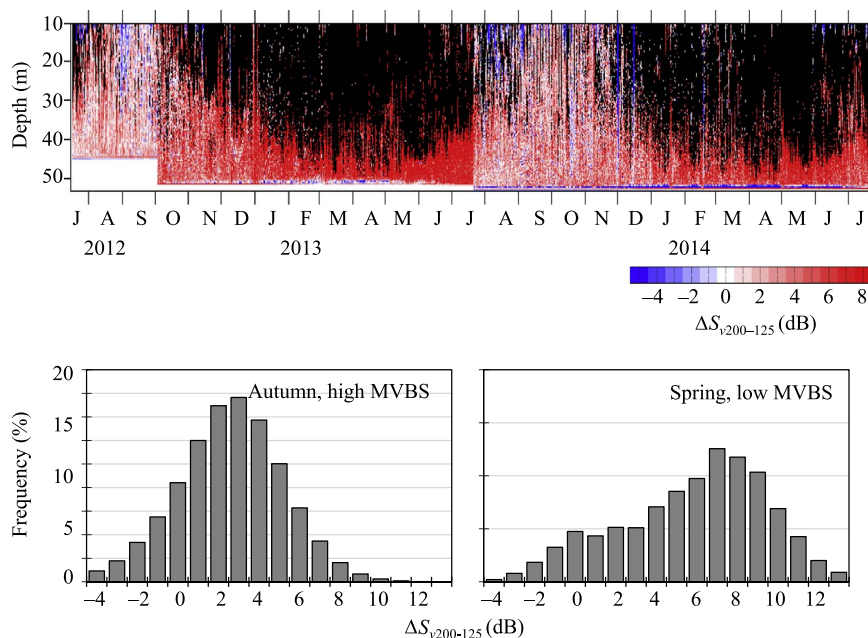


Fig. 9. An echogram of $\Delta S_{v,200-125}$ (S_v at 200 kHz – S_v at 125 kHz) (top panel), and histograms of $\Delta S_{v,200-125}$ in autumn with high mean volume backscattering strength (MVBS) (September–November 2013; bottom left) and in spring with low MVBS (March–May 2014; bottom right). Black areas in the echogram indicate that the signal-to-noise ratio is less than 10 dB and therefore $\Delta S_{v,200-125}$ is not available.

increase was probably important for the growth of zooplankton.

4.2. Current state of pelagic–benthic coupling in the southern Chukchi Sea

During the period of the spring phytoplankton bloom at the mooring site, zooplankton showed low biomass and were distributed in the lower water column without diel vertical migration; that is, there were temporal and spatial mismatches between zooplankton and phytoplankton production. Furthermore, the low water temperature during spring likely kept zooplankton grazing at a low level because rates of metabolic processes such as respiration increase with increasing water temperature (Alcaraz et al., 2013). Campbell et al. (2009) observed a low grazing impact of zooplankton on primary production during spring in the northern Chukchi Sea. Thus, most of the primary production during the spring phytoplankton bloom in the southern Chukchi Sea is available to sink to the bottom.

Large exports of carbon to the benthic food chain are possible not only during spring but also in other seasons. Nishino et al. (2016) reported an increase in turbidity with a decrease in dissolved oxygen in the bottom water during autumn at station SCH. They suggested that this was probably caused by advection and accumulation of particulate organic matter and its decomposition at the bottom at the mooring site in Hope Valley. Additionally, our acoustic observations suggest a decrease in populations of large Pacific zooplankton during winter. If this decrease indicates their unsuccessful overwintering, their carcasses must sink to the sea bottom. Recently, summertime zooplankton biomass, consisting primarily of Bering Sea species, was significantly higher compared to historical studies in the Chukchi Sea (Ershova et al., 2015). This increase could lead to an increased benthic carbon supply during winter due to increased numbers of sinking carcasses. As stated earlier, the pelagic processes suggest that pelagic–benthic coupling is still tight in the southern Chukchi Sea. From the perspective of benthic processes in the southern Chukchi Sea, sediment community oxygen consumption, which reflects the carbon supply to the benthos, and benthic biomass seem to have remained high between 2000 and 2010 compared to the 1980s (Grebmeier, 2012). Such observations suggest a tight pelagic–benthic coupling, that is consistent with the present study.

5. Conclusions

We followed the seasonal changes in zooplankton biomass in the southern Chukchi Sea using echo-sounder data from a two-year mooring. The seasonal peak in zooplankton biomass was in autumn whereas the minimum was in early spring; the seasonality did not correspond to that of phytoplankton productivity. This temporal mismatch suggests that (1) the seasonal zooplankton dynamics in the southern Chukchi Sea are less influenced by local growth of zooplankton during the spring phytoplankton bloom and more influenced by advection of zooplankton from the Bering Sea, and (2) most of the primary production during the spring phytoplankton bloom is available to sink to the bottom. The former observation is also supported by the nature of the main scatterers identified by using two sound frequencies: large zooplankton, believed to be Pacific species, dominate during the season with high zooplankton biomass. We also conclude that small zooplankton dominate in the seasons with low biomass. Observation (2) also suggests that there is still tight pelagic–benthic coupling in the southern Chukchi Sea. This tight coupling is consistent with the high benthic biomass reported for this area from the 1980s to 2010. The zooplankton seasonality described here will guide further research into the Arctic ecosystem, especially for that concerning animals at higher trophic levels, such as seasonally migrating seabirds and marine mammals.

Acknowledgements

We are grateful to the captains, crews, field technicians and other scientists onboard R/V *Mirai* and CCGS *Sir Wilfrid Laurier* for their successful deployments of moorings and for shipboard observations. Drs. M. Ito and E. Watanabe kindly provided satellite and bathymetry data. We also thank Drs. K. Matsuno and A. Yamaguchi for their zooplankton sampling around the mooring site onboard R/V *Mirai* and training ship (T/S) *Oshoro-Maru*. We are also grateful to anonymous reviewers, whose comments significantly improved the content of this manuscript. This study was supported by the Green Network of Excellence Program (GRENE Program) and Arctic Challenge for Sustainability (ArCS), which are funded by the Ministry of Education, Culture, Sports, Science and Technology of Japan.

References

- Alcaraz, M., Almeda, R., Saiz, E., Calbet, A., Duarte, C.M., Agusti, S., Santiago, R., Alonso, A., 2013. Effects of temperature on the metabolic stoichiometry of Arctic zooplankton. *Biogeosciences* 10, 689–697.
- Arrigo, K.R., Van Dijken, G., Pabi, S., 2008. Impact of a shrinking Arctic ice cover on marine primary production. *Geophys. Res. Lett.* 35, L19603. <http://dx.doi.org/10.1029/2008GL035028>.
- Ashjian, C.J., Campbell, R.G., Welch, H.E., Butler, M., Van Keuren, D., 2003. Annual cycle in abundance, distribution, and size in relation to hydrography of important copepod species in the western Arctic Ocean. *Deep-Sea Res. I* 50, 1235–1261.
- ASL Environmental Sciences, 2016. Scientific Post-processing of AZFP Data. (<http://www.aslenv.com/AZFP-data.html>) (last accessed 15.04.16).
- Astthorsson, O.S., Gislason, A., 1997. Biology of euphausiids in the subarctic waters north of Iceland. *Mar. Biol.* 129, 319–330.
- Berge, J., Cottier, F., Last, K.S., Varpe, Ø., Leu, E., Soreide, J., Eiane, K., Falk-Petersen, S., Willis, K., Nygård, H., Vogedes, D., Griffiths, C., Johnsen, G., Lorentzen, D., Brierley, A.S., 2009. Diel vertical migration of Arctic zooplankton during the polar night. *Biol. Lett.* 5, 69–72.
- Berge, J., Daase, M., Renaud, P.E., Ambrose, W.G., Jr., Darnis, G., Last, K.S., Leu, E., Cohen, J.H., Johnsen, G., Moline, M.A., Cottier, F., Varpe, Ø., Shunatova, N., Balazy, P., Morata, N., Massabuau, J.-C., Falk-Petersen, S., Kosobokova, K., Hoppe, C.J.M., Weslawski, J.M., Kuklinski, P., Legezynska, J., Nikishina, D., Cusa, M., Kedra, M., Wlodarska-Kowalczyk, M., Vogedes, D., Camus, L., Tran, D., Michaud, E., Gabrielsen, T.M., Granovitch, A., Gonchar, A., Krapp, R., Callesen, T.A., 2015. Unexpected levels of biological activity during the polar night offer new perspectives on a warming Arctic. *Curr. Biol.* 25, 1–7.
- Campbell, R.G., Sherr, E.B., Ashjian, C.J., Plourde, S., Sherr, B., Hill, V., Stockwell, D.A., 2009. Mesozooplankton prey preference and grazing impact in the western Arctic Ocean. *Deep-Sea Res. II* 56, 1274–1289.
- Carroll, M.L., Ambrose, W.G., Jr, Levin, B.S., Locke, W.L., Henkes, G.A., Hop, H., Renaud, P.E., 2011. Pan-Svalbard growth rate variability and environmental regulation in the Arctic bivalve *Serripes groenlandicus*. *J. Mar. Syst.* 88, 239–251.
- Chu, D., Ye, Z., 1999. A phase-compensated distorted wave Born approximation representation of the bistatic scattering by weakly scattering objects: application to zooplankton. *J. Acoust. Soc. Am.* 106, 1732–1743.
- Coachman, L.K., Aagaard, K., Tripp, R.B., 1975. Bering Strait: The Regional Physical Oceanography. Univ. Washington Press, Seattle, 175.
- Comiso, J.C., 2011. Large decadal decline of the Arctic multiyear ice cover. *J. Clim.* 25, 1176–1193.
- Conover, R.J., Siferd, T.D., 1993. Dark-season survival strategies of coastal zone zooplankton in the Canadian Arctic. *Arctic* 46, 303–311.
- Cottier, F.R., Tarling, G.A., Wold, A., Falk-Petersen, S., 2006. Unsynchronized and synchronized vertical migration of zooplankton in a high arctic fjord. *Limnol. Oceanogr.* 51, 2586–2599.
- Darnis, G., Robert, D., Pomerleau, C., Link, H., Archambault, P., Nelson, R.J., Geoffroy, M., Tremblay, J.-E., Lovejoy, C., Ferguson, S.H., Hunt, B.P.V., Fortier, L., 2012. Current state and trends in Canadian Arctic marine ecosystems: II. Heterotrophic food web, pelagic–benthic coupling, and biodiversity. *Clim. Change* 115, 179–205.
- De Robertis, A., Higginbottom, I., 2007. A post-processing technique to estimate the signal-to-noise ratio and remove echosounder background noise. *ICES J. Mar. Sci.* 64, 1282–1291.
- De Robertis, A., McKelvey, D.R., Ressler, P.H., 2010. Development and application of an empirical multifrequency methods for backscatter classification. *Can. J. Fish. Aquat. Sci.* 67, 1459–1474.
- Eisner, L., Hillgruber, N., Martinson, E., Maselko, J., 2013. Pelagic fish and zooplankton species assemblages in relation to water mass characteristics in the northern Bering and southeast Chukchi seas. *Pol. Biol.* 36, 87–113.
- Emery, W.J., Thomson, R.E., 2001. Profiling acoustic Doppler current meters. In: *Data Analysis Methods in Physical Oceanography*, Second and revised ed. Elsevier, Amsterdam, pp. 83–94.
- Ershova, E.A., Hopcroft, R.R., Kosobokova, K.N., Matsuno, K., Nelson, R.J., Yamaguchi, A., 2015. Long-term changes in summer zooplankton communities of the western Chukchi Sea. *Oceanography* 28, 100–115.
- Falk-Petersen, S., Hopkins, C.C.E., 1981. Ecological investigations on the zooplankton community of Balsfjorden, northern Norway: population dynamics of the euphausiids *Thysanoessa inermis* (Kroyer), *Thysanoessa raschii* (M. Sars) and *Meganycitiphanes norvegica* (M. Sars) in 1976 and 1977. *J. Plankton Res.* 3, 177–192.
- Falk-Petersen, S., Myzau, P., Kattner, G., Sargent, J.R., 2009. Lipids and life strategy of Arctic Calanus. *Mar. Boil. Res.* 5, 18–39.
- Fisher, J., Visbeck, M., 1993. Seasonal variation of the daily zooplankton migration in the Greenland Sea. *Deep-Sea Res. I* 40, 1547–1557.
- Fossheim, M., Primicerio, R., Johannessen, E., Invaldsen, R.B., Aschan, M.M., Dolgov, A.V., 2015. Recent warming leads to a rapid borealization of fish communities in the Arctic. *Nat. Clim. Change* 5, 673–677.
- Francois, R.E., Garrison, G.R., 1982. Sound absorption based on ocean measurements. Part II: boric acid contribution and equation for total absorption. *J. Acoust. Soc. Am.* 72, 1879–1890.
- Furusawa, M., 1988. Prolate spheroidal models for predicting general trends of fish target strength. *J. Acoust. Soc. Jpn.* 9, 13–14.
- Furusawa, M., Asami, T., Hamada, E., 1999. Detection range of echo sounders. In: *Proceedings of the 3rd JSPS International Seminar, Sustained Fishing Technology in Asia Towards the 21st Century*, pp. 207–213.
- Geinrikh, A.K., 2002. Life histories of the common copepods *Neocalanus flemingeri* and *Neocalanus plumchrus* in the west Bering Sea. *Oceanology* 42, 77–82.
- Grebmeier, J.M., 2012. Shifting patterns of life in the Pacific Arctic and subarctic seas. *Ann. Rev. Mar. Sci.* 4, 63–78.
- Grebmeier, J.M., McRoy, C.P., Feder, H.M., 1988. Pelagic–benthic coupling on the shelf of the northern Bering and Chukchi Seas. I. Food supply source and benthic biomass. *Mar. Ecol. Prog. Ser.* 48, 57–67.
- Grebmeier, J.M., Cooper, L.W., Feder, H.M., Sirenko, B.I., 2006a. Ecosystem dynamics of the Pacific-influenced northern Bering and Chukchi Seas in the Amerasian Arctic. *Prog. Oceanogr.* 71, 331–361.
- Grebmeier, J.M., Overland, J.E., Moore, S.E., Farley, E.V., Carmack, E.C., Cooper, L.W., Frey, K.E., Helle, J.H., McLaughlin, F.A., McNutt, S.L., 2006b. A major ecosystem shift in the northern Bering Sea. *Science* 311, 1461–1464.
- Hamilton, J.M., Collins, K., Prinsenberg, S.J., 2013. Links between ocean properties, ice cover, and plankton dynamics on interannual time scales in the Canadian Arctic Archipelago. *J. Geophys. Res.* 118, 5625–5639.
- Hass, C., Hendricks, S., Eicken, H., Herber, A., 2010. Synoptic airborne thickness surveys reveal state of Arctic sea ice cover. *Geophys. Res. Lett.* 37, L09501. <http://dx.doi.org/10.1029/2010GL042652>.
- Holliday, D.V., Pieper, R.E., Kleppel, G.S., 1989. Determination of zooplankton size and distribution with multifrequency acoustic technology. *J. Cons. Int. Explor. Mer.* 46, 52–61.
- Hopcroft, R.R., Kosobokova, K.N., Pinchuk, A.I., 2010. Zooplankton community patterns in the Chukchi Sea during summer 2004. *Deep-Sea Res. II* 57, 27–39.
- Hunt, G.L., Jr., Blanchard, A.L., Boveng, P., Dalpadado, P., Drinkwater, K.F., Eisner, L., Hopcroft, R.R., Kovacs, K.M., Norcross, B.L., Renaud, P., Reigstad, M., Renner, M., Skjoldal, H.R., Whitehouse, A., Woodgate, R.A., 2013. The Barents and Chukchi Seas: comparison of two Arctic shelf ecosystems. *J. Mar. Syst.* 109–110, 43–68.
- Kang, M., Furusawa, M., Miyashita, K., 2002. Effective and accurate use of difference in mean volume backscattering strength to identify fish and plankton. *ICES J. Mar. Sci.* 59, 794–804.
- Kobari, T., Ikeda, T., 1999. Vertical distribution, population structure and life cycle of *Neocalanus cristatus* (Crustacea: copepoda) in the Oyashio region, with notes on its regional variations. *Mar. Biol.* 134, 683–696.
- Kortsch, S., Primicerio, R., Beuchel, F., Renaud, P.E., Rodrigues, J., Lønne, O.J., Gulliksen, B., 2012. Climate-driven regime shifts in Arctic marine benthos. *Proc. Nat. Acad. Sci.* 109, 14052–14057.
- Kubilius, R., Ona, E., 2012. Target strength and tilt-angle distribution of the lesser sand eel (*Ammodytes marinus*). *ICES J. Mar. Sci.* 69, 1099–1107.
- Lavery, A.C., Wiebe, P.H., Stanton, T.K., Lawson, G.L., Benfield, M.C., Copley, N., 2007. Determining dominant scatters of sound in mixed zooplankton populations. *J. Acoust. Soc. Am.* 122, 3304–3326.
- Lawson, G.L., Wiebe, P.H., Ashjian, C.J., Gallager, S.M., Davis, C.S., Warren, J.D., 2004. Acoustically-inferred zooplankton distribution in relation to hydrography west of the Antarctic Peninsula. *Deep-Sea Res. II* 51, 2041–2072.
- Lawson, G.L., Wiebe, P.H., Ashjian, C.J., Chu, D., Stanton, T.K., 2006. Improved parameterization of Antarctic krill target strength models. *J. Acoust. Soc. Am.* 119, 232–242.
- Lemon, D., Johnston, P., Buermans, J., Loos, E., Borstad, G., Brown, L., 2012. Multiple-frequency moored sonar for continuous observations of zooplankton and fish. In: *Proceedings of Oceans 2012 MTS/IEEE, (Hampton Roads)*.
- Luo, J., Ortner, P.B., Forcucci, D., Cummings, S.R., 2000. Diel vertical migration of zooplankton and mesopelagic fish in the Arabian Sea. *Deep-Sea Res. II* 47, 1451–1473.
- Mackenzie, K.V., 1981. Nine-term equation for sound speed in the oceans. *J. Acoust. Soc. Am.* 70, 807–812.
- Marcus, N.H., 1984. Variation in the diapause response of *Labidocera aestiva* (Copepoda: calanoida) from different latitudes and its importance in the evolutionary process. *Biol. Bull.* 166, 127–139.
- Miller, C.B., Frost, B.W., Batchelder, H.P., Clemons, M.J., Conway, R.E., 1984. Life histories of large, grazing copepods in a subarctic ocean gyre: *Neocalanus plumchrus*, *Neocalanus cristatus*, and *Eucalanus bungii* in the northeast Pacific. *Prog. Oceanogr.* 13, 201–243.
- Nishino, S., Kikuchi, T., Fujiwara, A., Hirawake, T., Aoyama, M., 2016. Water mass characteristics and their temporal change in a biological hotspot in the southern Chukchi Sea. *Biogeosciences* 13, 2563–2578.
- Norrbin, M.F., 1994. Seasonal patterns in gonad maturation, sex ratio and size in some small, high-latitude copepods: implications for overwintering tactics. *J. Plankton Res.* 16, 115–131.
- Norrbin, M.F., 1996. Timing of diapause in relation to the onset of winter in the high-latitude marine copepods *Pseudocalanus acupes* and *Acartia longiremis*. *Mar. Ecol. Prog. Ser.* 142, 99–109.
- Pisareva, M.N., Pickart, R.S., Spall, M.A., Nobre, C., Torres, D.J., Moore, G.W.K., Whitedge, T.E., 2015. Flow of pacific water in the western Chukchi Sea: results from the 2009 RUSALCA expedition. *Deep-Sea Res. I* 105, 53–73.
- Purcell, J.E., Hopcroft, R.R., Kosobokova, K.N., Whitedge, T.E., 2010. Distribution, abundance, and predation effects of pelagic ctenophores and jellyfish in the western. *Arct. Ocean. Deep-Sea Res. II* 57, 127–135.
- Renaud, P.E., Morata, N., Carroll, M.L., Denisenko, S.G., Reigstad, M., 2008. Pelagic–benthic coupling in the western Barents Sea: processes and time scale. *Deep-Sea Res. II* 55, 2372–2380.
- Ronowicz, M., Kuklinski, P., Mapstone, G.M., 2015. Trends in the diversity, distribution and life history strategy of Arctic Hydrozoa (Cnidaria). *PLoS One* 10 (3), e0120204. <http://dx.doi.org/10.1371/journal.pone.0120204>.
- Smith, J.N., Ressler, P.H., Warren, J.D., 2010. Material properties of euphausiids and other zooplankton from the Bering Sea. *J. Acoust. Soc. Am.* 128, 2664–2680.
- Smith, S.L., Vidal, J., 1986. Variations in the distribution, abundance, and development

- of copepods in the southeastern Bering Sea in 1980 and 1981. *Cont. Shelf Res.* 5, 215–239.
- Springer, A.M., McRoy, C.P., Turco, K., 1989. The paradox of pelagic food webs in the northern Bering Sea - II. Zooplankton communities. *Cont. Shelf Res.* 9, 359–386.
- Stafford, K.M., Moore, S.E., Stabeno, P.J., Holliday, D.V., Napp, J.M., Mellinger, D.K., 2010. Biophysical ocean observation in the southeastern Bering Sea. *Geophys. Res. Lett.* 37, L02606. <http://dx.doi.org/10.1029/2009GL040724>.
- Stanton, T.K., Wiebe, P.H., Chu, D., Benfield, M.C., Scanlon, L., Martin, L., Eastwood, R.L., 1994. On acoustic estimates of zooplankton biomass. *ICES J. Mar. Sci.* 51, 505–512.
- Steele, M., Ermold, W., Zhang, J., 2008. Arctic ocean surface warming trends over the past 100 years. *Geophys. Res. Lett.* 35, L02614. <http://dx.doi.org/10.1029/2007GL031651>.
- Volkov, A.F., 2008. Mean annual characteristics of zooplankton in the Sea of Okhotsk, Bering Sea and northwestern Pacific (annual and seasonal biomass values and predominance). *Russ. J. Mar. Biol.* 34, 437–451.
- Wallace, M.I., Cottier, F.R., Berge, J., Tarling, G.A., Griffiths, C., Brierley, A.S., 2010. Comparison of zooplankton vertical migration in an ice-free and a seasonally ice-covered Arctic fjord: an insight into influence of sea ice cover on zooplankton behavior. *Limnol. Oceanogr.* 55, 831–845.
- Wassmann, P., Duarte, C.M., Agustí, S., Sejrl, M.K., 2011. Footprints of climate change in the Arctic marine ecosystem. *Glob. Change Biol.* 17, 1235–1249.
- Weingartner, T.J., 1997. A review of the physical oceanography of the northeastern Chukchi Sea. In: Reynolds, J. (Ed.), *Fish Ecology in Arctic North America* 19. American Fisheries Society Symposium, Bethesda, Maryland, 40–59.
- Weingartner, T.J., Danielson, S., Sasaki, Y., Pavlov, V., Kulakov, M., 1999. The Siberian Coastal Current: a wind- and buoyancy-forced Arctic coastal current. *J. Geophys. Res.* 104, 29697–29713.
- Yamamoto-Kawai, M., McLaughlin, F.A., Carmack, E.C., Nishino, S., Shimada, K., Kurita, N., 2009a. Surface freshening of the Canada Basin, 2003–2007: river runoff versus sea ice meltwater. *J. Geophys. Res.* 114, C00A05. <http://dx.doi.org/10.1029/2008JC005000>.
- Yamamoto-Kawai, M., McLaughlin, F.A., Carmack, E.C., Nishino, S., Shimada, K., 2009b. Aragonite undersaturation in the Arctic Ocean: effects of ocean acidification and sea ice melt. *Science* 326, 1098–1100.
- Yasuma, H., Nakagawa, R., Yamakawa, T., Miyashita, K., Aoki, I., 2009. Density and sound-speed contrasts, and target strength of Japanese sand eel *Ammodytes personatus*. *Fish. Sci.* 75, 545–552.